ELSEVIER

Contents lists available at ScienceDirect

Journal of Quantitative Spectroscopy & Radiative Transfer

journal homepage: www.elsevier.com/locate/jqsrt



Application of the scaling approach to particles having simple, fundamental shapes, in the Rayleigh-Debye-Gans diffraction limit



Justin B. Maughan*, Christopher M. Sorensen

Department of Physics, Kansas State University, Manhattan, KS 66506, USA

ARTICLE INFO

Article history:
Received 14 July 2018
Revised 23 October 2018
Accepted 23 October 2018
Available online 25 October 2018

ABSTRACT

Presented is a scaling approach for understanding features, such as power laws and crossover points, of the light scattered in the $m \to 1$, $\rho = 2kR_{\rm veq}|m-1| < 1$, Rayleigh-Debye-Gans diffraction limit. The scaling approach is based on comparison of the length scale of the scattering, which is the inverse of the scattering wave vector, and the various length scales of the scattering entity. It will be shown that the scaling approach correctly predicts the exponents of the power law regions and the locations of the first and second Guinier regimes which define the boundaries of the power laws. Furthermore, the scaling approach yields a semi-quantitative prediction of the coefficients of the power laws. These Guinier boundaries and power law coefficients are described by a single parameter, the aspect ratio of the scattering object.

© 2018 Elsevier Ltd. All rights reserved.

1. Introduction

An immense amount of work has been done over the last century in the area of scattering. There are typically two main questions researchers seek to discover. How does a particular particle or collection of particles scatter electromagnetic waves, and can information about the particle or particles be extracted from the scattered intensity? This work will focus on the former in the $m \rightarrow 1$, $\rho = 2kR_{\text{veq}}|m-1| < 1$, Rayleigh–Debye–Gans diffraction (RDG) limit [1], where m is the relative index of refraction, ρ is the phase shift parameter, k is magnitude of the incident wave vector, and R_{veg} is the radius of a sphere with equivalent volume. Much of the previous work on diffractive scattering has been done in the area of small angle X-ray scattering to which the anomalous diffraction approximation is applicable. A focus of past work has been to understand how to calculate the structure factor of a given particle or collection of particles. The structure factor describes the angular behavior of scattering in the RDG limit, and is solely dependent on the particles shape, and relative orientations of the particles being considered [2].

The structure factor is given by the Fourier transform of real space structure of the particle squared [3]. For simpler particle shapes, such as a sphere, the Fourier transform can be calculated analytically [1]. As the geometry of the particle becomes more complex, the integrals that need to be evaluated become increasingly more complicated, and in many cases must be computed

numerically [3]. Guinier and Fournet put forth a semi-quantitative approach for calculating the average behavior of the structure factor for an arbitrary, three-dimensional, homogeneous particle [4]. For any shape of a particle, Guinier and Fournet give that the structure factor in the large scattering wave vector limit as

$$S(q) = \frac{2\pi N^2 S}{V^2} q^{-4} \tag{1}$$

where N is the number of point scatterers within the particle, S without an argument of q is the surface area, not to be confused with the structure factor which will always be presented as S(q), V is the volume and q is the magnitude of the scattering wave vector and has units of inverse length. The q^{-4} dependence in Eq. (1) is known as Porod's law [4]. Subsequent work has been done with the light scattered by fractal aggregates [5] and Porod's law has been generalized to

$$S(q) \propto q^{-(2D_m - D_s)} \tag{2}$$

where D_m is the mass scaling dimension and D_s is the surface scaling dimension. Note that for a non-fractal three-dimensional object, $D_m = 3$ and $D_s = 2$ yield an exponent of -4 in Eq. (2) consistent with Eq. (1).

The scaling approach to be presented here is also a semiquantitative approach for calculating the structure factor. The scaling approach can be applied to particles of any dimension including fractal aggregates, which have non-integer scaling dimensions, and is applicable to both homogeneous and non-homogeneous particles [6,7]. In this work we extend the treatment first presented in [6]. While the main focus of Oh and Sorensen [6] was on fractal aggregates, the focus of this work will be on three-dimensional

^{*} Corresponding author. E-mail address: maughan@phys.ksu.edu (J.B. Maughan).

homogeneous particles, with results nearly identical to the work of Guinier and Fournet.

Some favorable attributes of the scaling approach are that it relies on a comparison of the length scale of the scattering measurement q^{-1} to length scales of the scattering object. These comparisons give physical insight to the scattering measurement. Also, when a particle has an aspect ratio much greater than or much less than unity, the scattering pattern will exhibit two distinct power law regions. The large q power law behavior is given by Porod's law as presented in Eq. (2). There will also be an intermediate qpower law region where Porod's law is not applicable [8]. Guinier and Fournet only come by this intermediate q power law region by using a different method for approximating the Fourier transform that resulted in Eq. (1). Beaucage has put forth a unified exponential approach for calculating both the intermediate and large q power law regions [8]. In the unified exponential approach, a sum of exponential terms is used for the approximation, requiring nine parameters to calculate the structure factor. The scaling approach on the other hand only requires the geometric parameters of the particle. It will be shown here that the scaling approach captures the correct power laws in both the intermediate and high q power law regions, as well as the coefficients to these power laws, and can be expressed solely in terms of the aspect ratio. The scaling approach is also able to predict the crossover points between these distinct power law regions and express them in terms of the aspect ratio.

2. The scaling approach

In the scaling approach the scattering volume or particle is considered to be made up of N identical point scatterers. The discretization of the volume is used as opposed to a continuous integral to allow for more arbitrarily shaped particles, and those with fluctuations in density, to be considered [6]. While the structure factor for particles with simple geometric shapes such as spheres and cylinders can be calculated by taking the continuous integral of the volume, the integration of the volume becomes increasingly difficult for more complex particles, or systems of particles such as the fractal aggregates considered in [6,9]. By discretizing the volume of the particles, it allows for a more robust and universal approach.

The structure factor provides information about the structure of the system and the angular behavior of the scattering from the N point scatterers. The structure factor can be calculated as a double sum over the positions of the N point scatterers and is given by $\lceil 10 \rceil$

$$S(\vec{q}) = \sum_{l,j}^{N} e^{i\vec{q}\cdot(\vec{r}_l - \vec{r}_j)} \tag{3}$$

where i is the complex value $\sqrt{-1}$. The \vec{r}_l and \vec{r}_j are the positions of the lth and jth scatterers. The scattering wave vector \vec{q} is given by

$$\vec{q} = \vec{k}_{\text{sca}} - \vec{k}_{\text{inc}} \tag{4}$$

where \vec{k}_{sca} is the scattered wave vector, and \vec{k}_{inc} is the incident wave vector. Only elastic scattering will be considered in which case $|\vec{k}_{\text{sca}}| = |\vec{k}_{\text{sca}}| = k = 2\pi/\lambda$ and λ is the wavelength. The magnitude of \vec{q} is given by

$$q = 2k\sin\left(\theta/2\right) \tag{5}$$

where θ is the scattering angle.

The application of the scaling approach considers an ensemble of particles randomly oriented, or a single particle orientationally averaged, thus $S(\vec{q}) = S(q)$. Also, polarization effects are ignored, treating the waves as scalars. This is on par with treating

the waves as having a polarization perpendicular to the scattering plane defined by $\vec{k}_{\rm sca}$ and $\vec{k}_{\rm inc}$ and considering multiple scattering not to be significant [6]. It can be seen from Eq. (5) that the scattering wave vector q has units of inverse length, thus q^{-1} is the inherent length scale of the scattering. By comparing the length scales of the system of point scatterers and q^{-1} , the double sum can be determined to either add up in phase coherently or randomly. For a system of N scatterers there are two limiting cases [6,7]:

- 1. If the N point scatterers are within q^{-1} of each other, the phases of the N scattered waves will be essentially the same, hence the waves will add constructively. Then the total scattered amplitude will be proportional to N. The intensity, which is proportional to the structure factor, goes as the square of the amplitude and hence will be proportional to N^2 .
- 2. If the N point scatterers have all possible pairs separated by a distance greater than q^{-1} , the waves will add up randomly. The total scattered amplitude in this case will be proportional to \sqrt{N} , and the total scattered intensity will be proportional to N.
- 3. Only when there are fluctuations in the density will there be a nonzero contribution to the scattering at scattering angles other then $\theta=0$. This is a consequence of the Ewald–Oseen extinction theorem [11,12]. This means, for example, that for an inhomogeneous particle the scattering will come from both the discontinuity at the surface of the particle and from any inhomogeneities in the bulk. For a homogeneous particle the scattering comes purely from the discontinuity at the surface of the particle.

3. Application of the scaling approach

We will determine the rotationally averaged structure factor for a variety of particles. To do this we consider that instead of the particle taking on many different orientations, the q-vector is rotated through all possible orientations forming spherical q-regions of radius q^{-1} . As q^{-1} has units of length, when q is small these spherical q-regions will be large, and the entire particle will lie within a single q-region as in Fig. 1a. As q increases, the q-regions will become smaller, and the particle will be covered by multiple q-regions as in Fig. 1b. The N_q point scatterers within a q-region will be within q^{-1} of each other, and the sum of their scattered waves squared will be N_q^2 (situation 1 above). The n_q q-regions will be separated from each other by more than q^{-1} and the sum of their scattered waves squared from the q-regions will be n_q (situation 2 above). The total structure factor will then be given by

$$S(q) = N_a^2 n_a. (6)$$

When considering only homogeneous particles, the scattering will come purely from the discontinuity at the surface (statement 3 above), so only the n_q q-regions that contain part of the particles surface need to be considered in Eq. (6).

When the aspect ratio is close to unity and q^{-1} is larger than D/2 where D is the dimension describing the size of the particle, the entire particle will lie within a single q-region and $S(q) = N^2$. For example, D would be 2R the diameter of a cylinder where R is the radius or the length L as both are equal when the aspect ratio $\varepsilon = \frac{L}{2R} = 1$. As q^{-1} decreases and becomes less than D/2 the particle will have q-regions that contain part of the particle's surface as in Fig. 1b. In this case n_q will be given by

$$n_q = \frac{\text{surface area of the particle}}{\text{cross section of a } q - \text{region}} = \frac{S}{\pi q^{-2}}.$$
 (7)

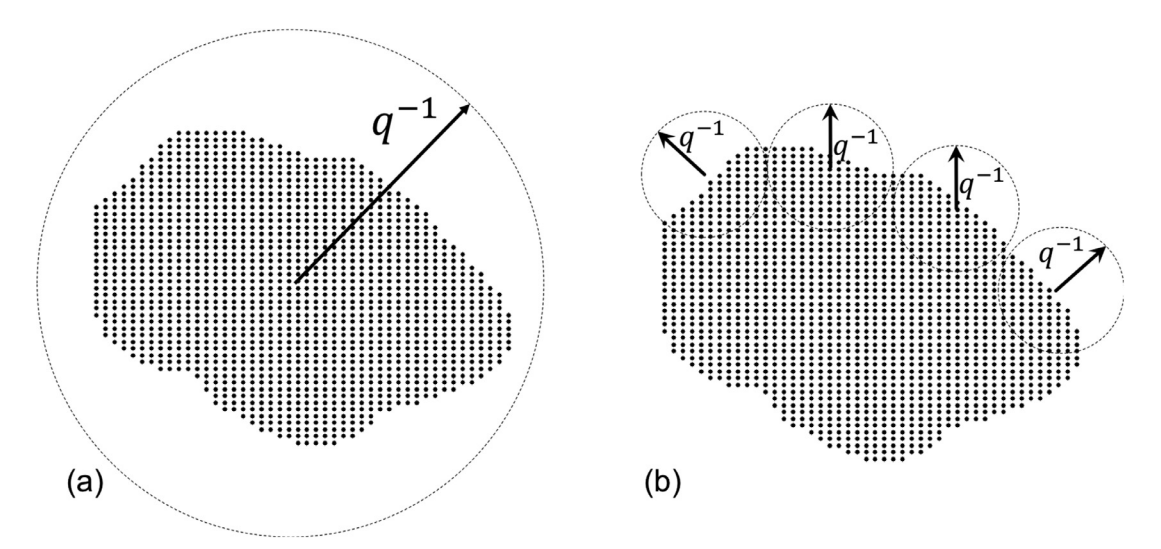


Fig. 1. A particle discretized into Npoint scatterers. (a) The entire particle fits within a single q-region. (b) Several q-regions cover the surface of the particle.

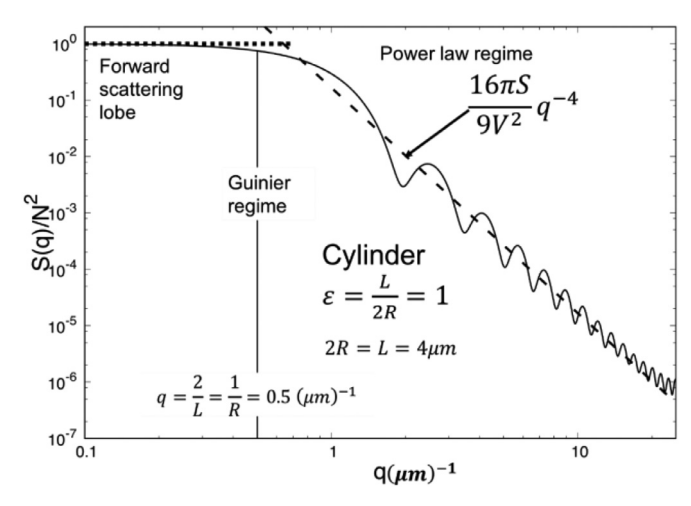


Fig. 2. The structure factor for a cylinder. The solid black curve shows the Fourier transform numerically calculated using Eq. (1). The dashed line is computed using the scaling approach.

The number of point scatterers within a q-region will be given by

$$N_q = \text{density of points} \times \text{volume of a } q - \text{region} = \left(\frac{N}{V}\right) \frac{4}{3}\pi q^{-3}.$$
(8)

Putting together Eqs. (6)–(8) we get that the structure factor when q^{-1} is smaller than D/2 will go as

$$S(q) = \frac{16\pi N^2 S}{9V^2} q^{-4}. (9)$$

This compares well to the semi-quantitative result of Eq. (1).

To demonstrate that Eq. (9) describes the normalized structure factor, Fig. 2 shows the structure factor of a cylinder calculated using Eq. (3) plotted vs. q. From Fig. 2a picture of the scattering can now be put together. In the forward scattering lobe, q is small and thus q^{-1} is large, the scattering is constant in q and goes as N^2 . As q increases and approaches 2/D (D=L=2R), the scattering begins to fall off and crosses over into the power law regime described by Eq. (9). This crossover regime is known as the Guinier regime, from which particle size can be retrieved [13]. Eq. (9) has three extensive quantities, N, V, and S. However, N^2/V^2 is the density squared,

which is an intensive quantity. Hence, the only remaining extensive dependence lies with the surface area S. This fact emphasizes that the scattering intensity in the large q regime is a consequence of the inhomogeneity of the scatterer at the surface S.

Typically, it is more advantageous to plot the structure factor vs. a dimensionless parameter. To do this, Eq. (9) can be multiplied and divided by $R_{\rm veq}^4$. The structure factor for the power law region can then be expressed as

$$S(q) = \frac{16\pi N^2 S R_{\text{veq}}^4}{9V^2} (q R_{\text{veq}})^{-4}.$$
 (10)

Not only does this provide a dimensionless parameter to plot against but also a dimensionless coefficient. Eq. (10) can also be expressed as

$$S(q) = \frac{4N^2S}{S_{\text{veq}}} (qR_{\text{veq}})^{-4}$$
 (11)

where S_{veq} is the surface area of a sphere with the same volume. The coefficient in Eq. (11) again demonstrates the structure factor's dependence on the surface of the particle in the large q regime.

For the four different particle shapes that will be considered in this work (cylinders, hexagonal columns, square columns, and spheroids), the dimensionless coefficient can be expressed solely in terms of ε . The crossover point in the Guinier regime can also be expressed solely in terms of ε , thus allowing the scattering to be described by a single parameter. Fig. 3 shows the structure factor plotted vs. $qR_{\rm veq}$ for the four particle shapes being considered. The crossover point as well as the dimensionless coefficients have all been expressed in terms of ε . Although in Fig. 3, $\varepsilon=1$, the expressions for the coefficients hold for all values of ε in the large q regime. The expressions for the crossover points will hold for values close to unity. Once the aspect ratio begins to move away from unity, either larger or smaller, the crossover points will begin to separate as the intermediate power law regime emerges.

If the aspect ratio is much greater than, or much less than unity, there will be two Guinier regimes and two power law regimes. The first Guinier regime will occur when q^{-1} crosses through half the largest dimension describing the particle $D_1/2$. The second will occur when q^{-1} crosses through half the second dimension describing the particle $D_2/2$. Continuing to use a cylinder as an example, when $= L/2R \gg 1$, $D_1 = L$ and $D_2 = 2R$ as shown in Fig. 4. As with any particle, when q^{-1} is larger than $D_1/2$, i.e. L/2 for a long cylinder, the scattering will go as N^2 .

As q^{-1} becomes smaller with increasing q, it first passes through $D_1/2$, i.e. L/2 for a long cylinder, but remains larger than

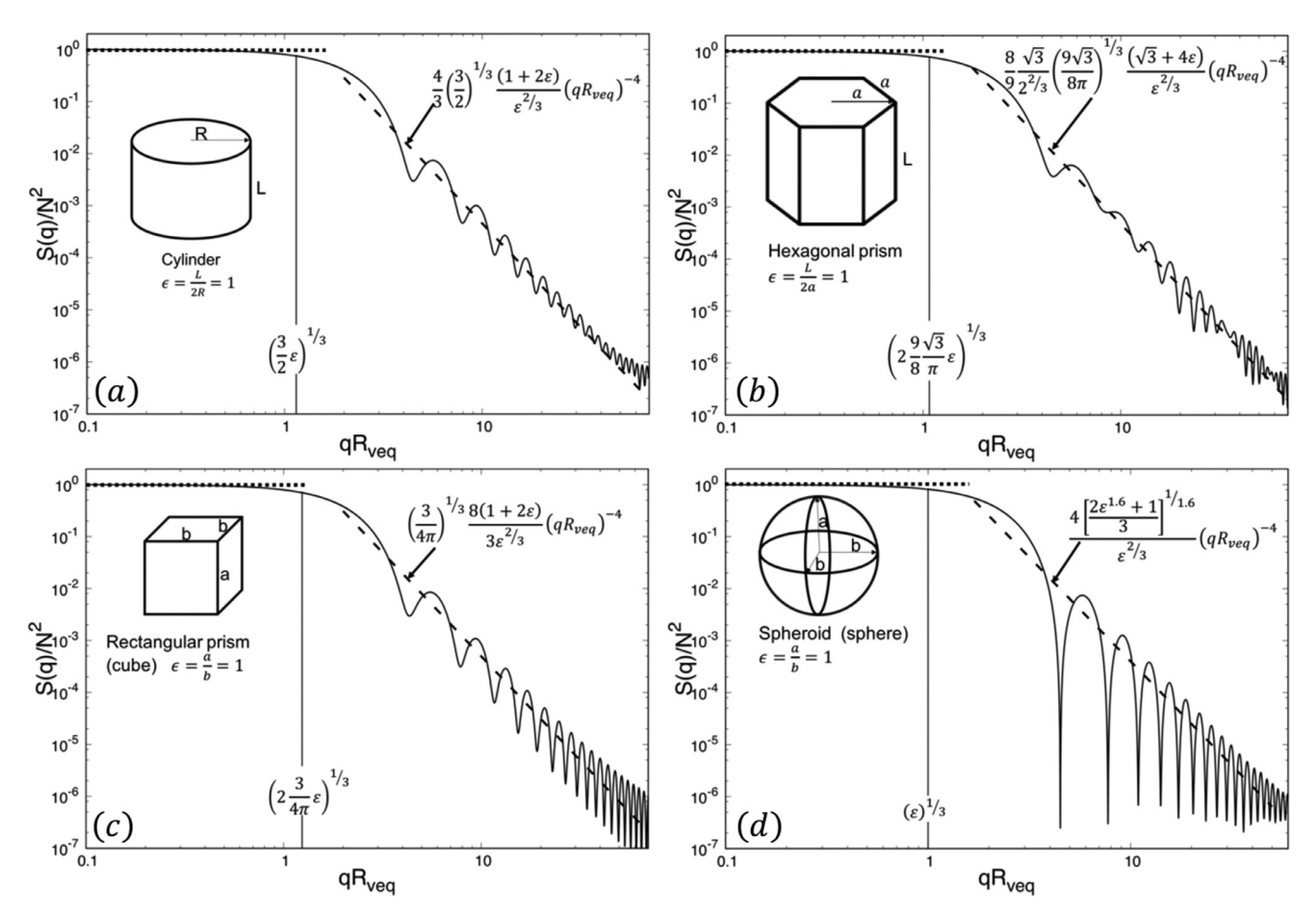


Fig. 3. The structure factor for a cylinder, (a), hexagonal prism (b), rectangular prism (c), and a spheroid (d) all with $\varepsilon = 1$. The solid black curve shows the Fourier transform numerically calculated using Eq. (3). The dashed lines are computed using the scaling approach. The formulas including the parameter ε are calculated using Eq. (10).

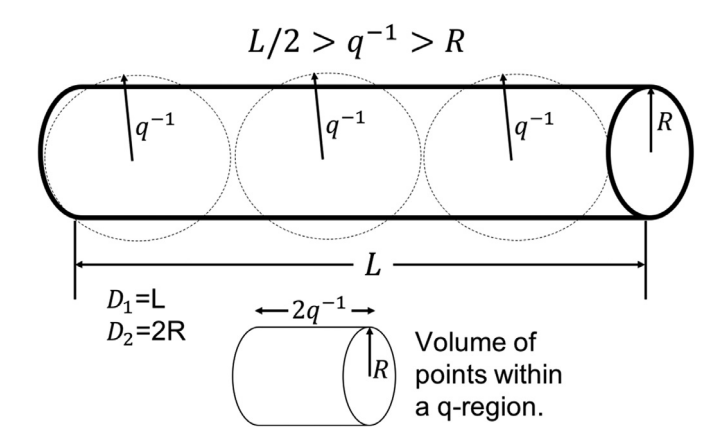


Fig. 4. A cylinder with $\varepsilon = L/2R = 10$. A finite number of q-regions fit within L, while all the q-regions overlap in R. The volume of a q-region can be approximated as smaller cylinders, as drawn below.

 $D_2/2$, i.e. R for a long cylinder. In this range of q the q-regions will overlap the particle in the $D_2/2$, i.e. R for a long cylinder, direction, but there will be a finite number that lie within the $D_1/2$, i.e. L/2 for a long cylinder, direction as shown in Fig. 4. The number of q-regions will therefore be set by how many can fit within the largest dimension of the particle D_1 , i.e. L for a long cylinder. Taking D_1 divided by the diameter of a q-region leads to n_q which can be expressed as

$$n_q = \frac{D_1}{2q^{-1}} \ \varepsilon \gg 1 \ \frac{D_2}{2} < q^{-1} < \frac{D_1}{2}.$$
 (12)

The number of point scatterers in each q-region will be determined by D_2 , i.e. R for a long cylinder. As shown in Fig. 4, the section of each q-region that lies within the particle can be approximated as a small cylinder with a length given by the diameter of a q-region $2q^{-1}$. The number of scatters in the q-region will then be given by the product of the density of point scatterers, diameter of a q-region, and the cross-sectional area of the cylinder described by D_2 , i.e. R for a long cylinder, and is expressed as

$$N_q = \frac{N}{V} C_{D_2} 2q^{-1} \ \varepsilon \gg 1 \ \frac{D_2}{2} < q^{-1} < \frac{D_1}{2}. \tag{13}$$

where C_{D_2} is the cross-sectional area described by D_2 . For example, in the case of a circular cylinder this would be πR^2 .

Putting together Eqs. (6), (12) and (13) we arrive at an expression for the structure factor in this intermediate regime

$$S(q) = 2\frac{N^2}{V^2}C_{D_2}^2D_1q^{-1} \ \varepsilon \gg 1 \ \frac{D_2}{2} < q^{-1} < \frac{D_1}{2}. \tag{14}$$

In Eq. (14) we see that there is a power law of -1. Finally, as the radius of q-regions become smaller than $D_2/2$, i.e. R for a long cylinder, there is a second Guinier regime and the scattering is again described by Eq. (9). Plotting vs. the dimensionless parameter qR_{veq} and expressing all coefficients and crossover points in terms of ε is shown in Fig. 5 for a long cylinder, long hexagonal columns, long square columns, and prolate spheroids.

Now to consider the other extreme, with $\varepsilon \ll 1$ as shown in Fig. 6 and continuing with the use of a circular cylinder as an example which we now transform to a disk. In this case $D_1 = 2R$ and $D_2 = L$. The concepts laid out for when $\varepsilon \gg 1$ are similar, except that as q^{-1} grows smaller with increasing q it will pass through

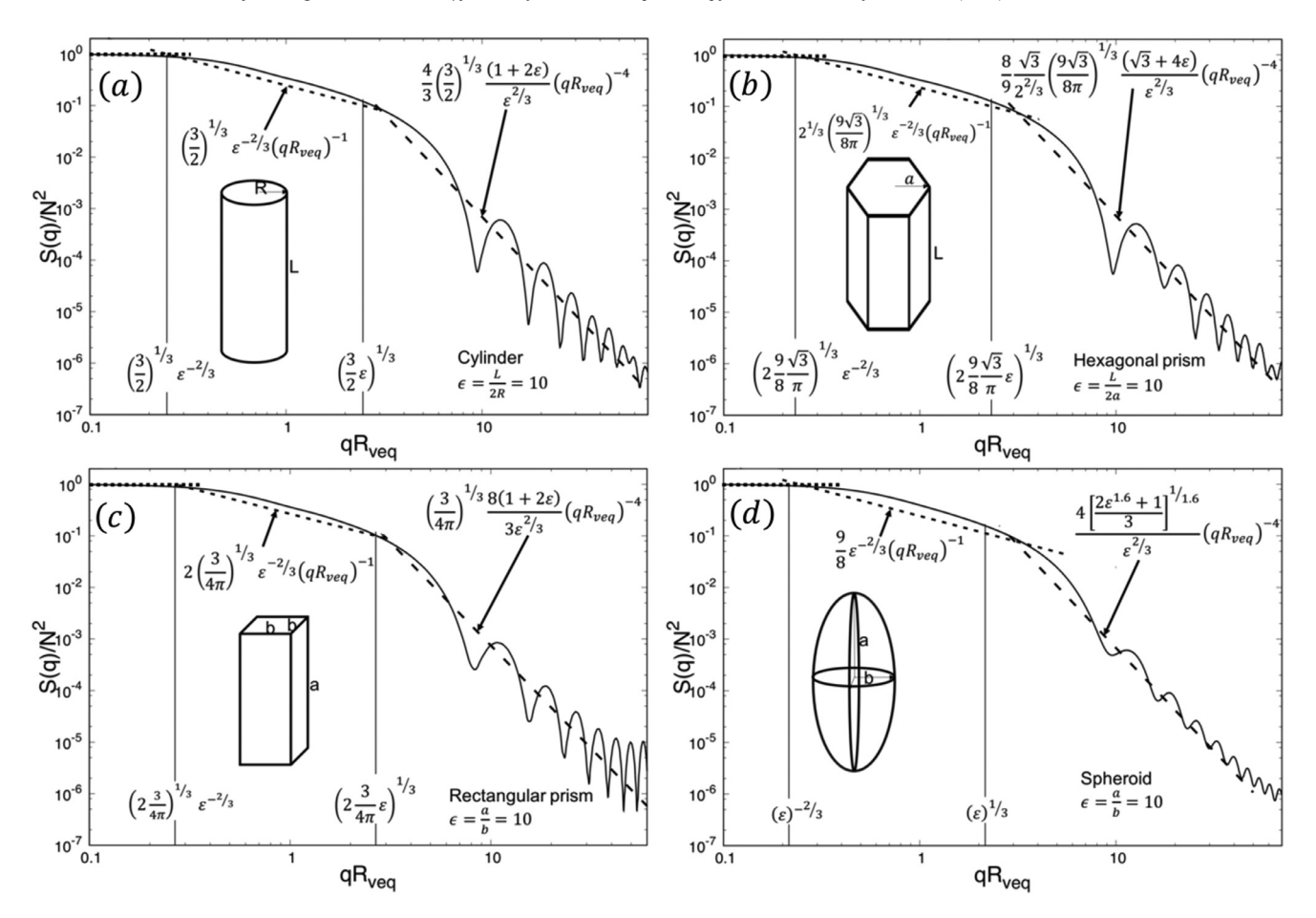


Fig. 5. The structure factor for a circular cylinder (a), hexagonal prism (b), rectangular prism (c), and a prolate spheroid (d) all with $\varepsilon = 10$. The solid black curve shows the Fourier transform numerically calculated using Eq. (3). The dashed lines are computed using the scaling approach. The formulas including the parameter ε in the intermediate q regime are calculated using Eq. (14), and in the large q regime using Eq. (10).

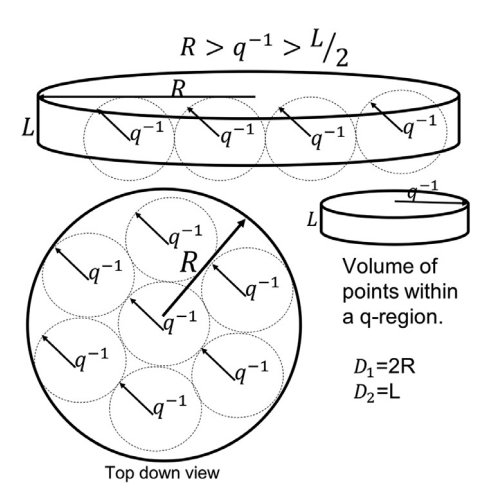


Fig. 6. A circular disk with $\varepsilon = L/2R = 0.1$. A finite number of q-regions fit within R, while all the q-regions overlap in L. The volume of a q-region can be approximated as smaller disks.

the larger R first instead of L/2. This leads to spherical q-spaces extending beyond the particle in the smaller L direction while a finite number fit within the area of the R direction as shown in Fig. 6. The number of q-regions will therefore be set by the ratio of the cross-sectional area described by $D_1 = 2R$, and the cross-sectional

area of a q-region, πq^{-2} , expressed as

$$n_q = \frac{C_{D_1}}{\pi a^{-2}} \ \varepsilon \ll 1 \ \frac{D_2}{2} < q^{-1} < \frac{D_1}{2}. \tag{15}$$

The number of point scatterers within a q-region will again be given by the product of the density of point scatterers and the volume of a q-region that lies within the particle. In the $\varepsilon \ll 1$ limit we can again approximate the section of each q-region that lies within the particle as a disk, also shown in Fig. 6. The thickness of the disk will be given by L and the radius of the disk will be given by L and the radius of the disk will be given by L and the radius of the disk will be given by L and the radius of the disk will be given by L and the radius of the disk will be given by L and the radius of the disk will be given by L and the radius of the disk will be given by L and the radius of the disk will be given by L and the radius of the disk will be given by L and the radius of the disk will be given by L and the radius of the disk will be given by L and L are the radius of the disk will be given by L and L are the radius of the disk will be given by L and the radius of the disk will be given by L and the radius of the disk will be given by L and the radius of the disk will be given by L and the radius of the disk will be given by L and the radius of the disk will be given by L and the radius of the disk will be given by L and the radius of the disk will be given by L and the radius of the disk will be given by L and the radius of the disk will be given by L and the radius of the disk will be given by L and L are the radius of the disk will be given by L and L are the radius of the disk will be given by L and L are the radius of the disk will be given by L and L are the radius of the disk will be given by L and L are the radius of the disk will be given by L and L are the radius of the disk will be given by L and L are the radius of L are the radiu

$$N_q = \frac{N}{V} D_2 \pi q^{-2} \ \varepsilon \ll 1 \ \frac{D_2}{2} < q^{-1} < \frac{D_1}{2}. \tag{16}$$

Putting together Eqs. (6), (15), and (16) we arrive at an expression for the structure factor in this intermediate regime

$$S(q) = \pi \frac{N^2}{V^2} C_{D_1} D_2^2 q^{-2} \ \varepsilon \ll 1 \ \frac{D_2}{2} < q^{-1} < \frac{D_1}{2}. \tag{17}$$

In equation Eq. (17) we see that there is a power law of -2. Finally, as the radius of q-regions become smaller than $D_2/2$, i.e. L/2 for disks, with increasing q, there is a second Guinier regime and the scattering is again described by Eq. (9). Plotting vs. the dimensionless parameter $qR_{\rm veq}$ and expressing all coefficients and crossover points in terms of ε is shown in Fig. 7 for a disk, flat hexagonal column, flat square column, and an oblate spheroid.

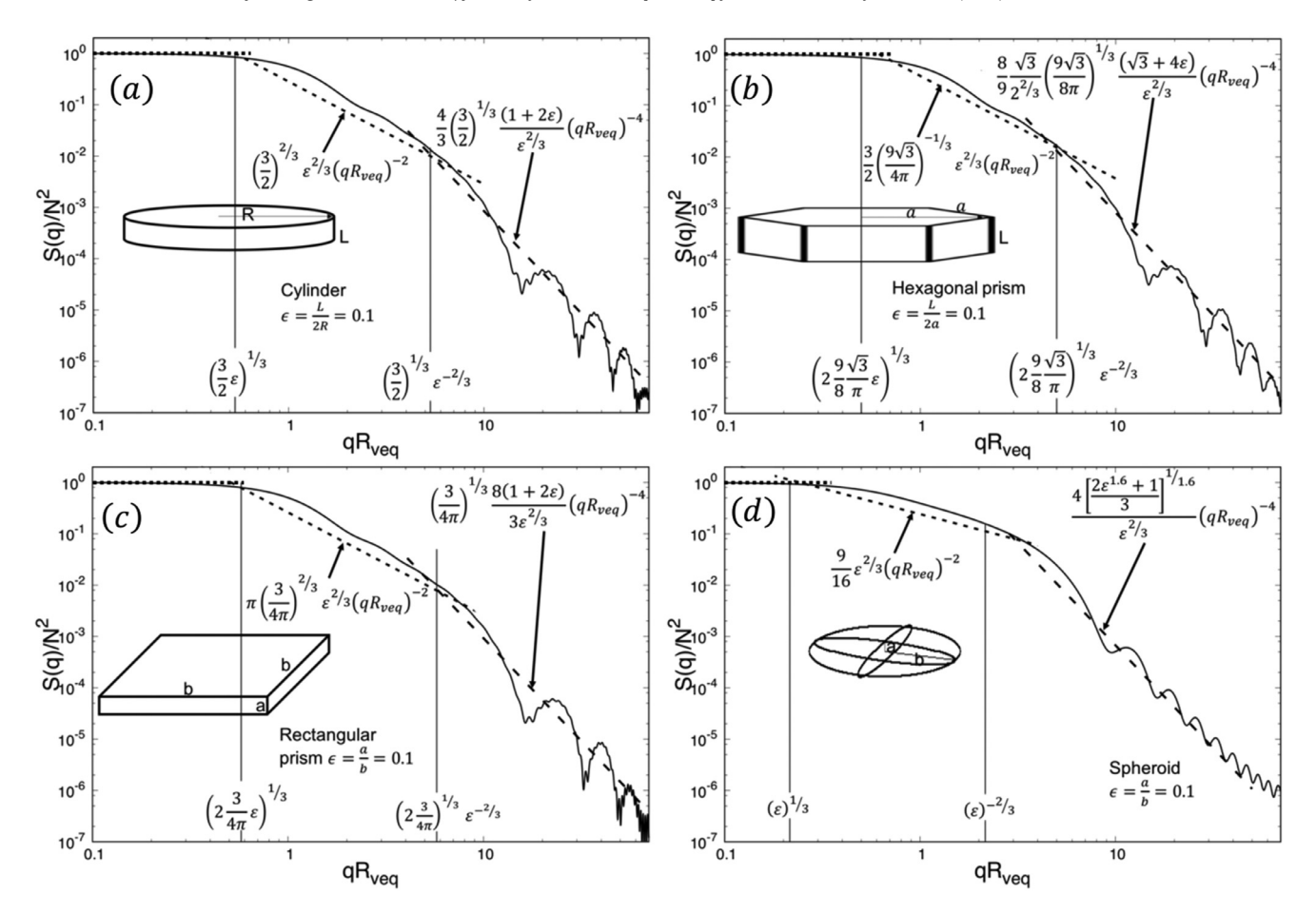


Fig. 7. The structure factor for a disk (a), a flat hexagonal prism (b), a flat rectangular prism (c), and a spheroid (d) all with $\varepsilon = 0.1$. The solid black curve shows the Fourier transform numerically calculated using Eq. (3). The dashed lines are computed using the scaling approach. The formulas including the parameter ε in the intermediate q regime are calculated using Eq. (17), and in the large q regime using Eq. (10).

4. Conclusion

Figs. 3, 5, and 7 demonstrate that the scaling approach is an effective semi-quantitative approach to describe scattering in the *RDG* limit. The scaling approach correctly predicts the exponents and the locations of the first and second Guinier regimes. It also yields a semi-quantitative prediction of the coefficients of the power laws. The positions of the Guinier regimes, and the coefficients of the power laws are solely dependent on one parameter, the aspect ratio of the scattering object ε , when the structure factor is plotted versus the dimensionless $qR_{\rm veq}$. However, the scaling approach is not capable of capturing the ripple structure of the structure factor and only predicts the average. Finally, the scaling approach lends physical insight into the scattering process by application of q^{-1} as the length scale of the scattering process, and the concept that only changes in density scatter waves.

Acknowledgment

This work was supported by NSF grant AGS 1649783.

References

- [1] van de Hulst HC. Light scattering by small particles. corrected edition. New York: Dover Publications; 1981.
- [2] Jackson JD. Classical electrodynamics. 3rd ed. New York: Wiley; 1999.
- [3] Feğgin LA, Svergun DI, Taylor GW. Structure analysis by small-angle x-ray and neutron scattering. New York: Plenum Press; 1987.
- [4] Guinier A. Small-angle scattering of X-rays. Wiley; 1955.
- [5] Martin JE, Hurd AJ. Scattering from fractals. J Appl Crystallogr 1987;20:61–78. doi:10.1107/S0021889887087107.
- [6] Oh C, Sorensen CM. Scaling approach for the structure factor of a generalized system of scatterers. J Nanoparticle Res 1999;1:369-77. doi:10.1023/A: 1010033111039.
- [7] Sorensen CM. Light scattering by fractal aggregates: a review. Aerosol Sci Technol 2001;35:648–87. doi:10.1080/02786820117868.
- [8] Beaucage G. Approximations leading to a unified exponential/power-law approach to small-angle scattering. J Appl Crystallogr 1995;28:717–28. doi:10.1107/S0021889895005292.
- [9] Sorensen CM, Yon J, Liu F, Maughan J, Heinson WR, Berg MJ. Light scattering and absorption by fractal aggregates including soot. J Quant Spectrosc Radiat Transf 2018;217:459–73. doi:10.1016/j.jqsrt.2018.05.016.
- [10] Jackson JD. Classical electrodynamics. 3rd ed. New York: Wiley; 1998.
- [11] Born M. Principles of optics: electromagnetic theory of propagation, interference and diffraction of light. 6th ed. Oxford, New York: Pergamon Press; 1980.
- [12] Eugene. Hecht. Optics. 4th ed. Reading, MA: Addison-Wesley; 2002.
- [13] Heinson YW, Maughan JB, Heinson WR, Chakrabarti A, Sorensen CM. Light scattering Q-space analysis of irregularly shaped particles. J Geophys Res Atmos 2016;121:682–91. doi:10.1002/2015JD024171.